HHS Public Access

Author manuscript

Shock. Author manuscript; available in PMC 2019 May 28.

Published in final edited form as:

Shock. 2019 May ; 51(5): 569–579. doi:10.1097/SHK.0000000000001300.

Burn-induced Microglia Activation is Associated with Motor Neuron Degeneration and Muscle Wasting in Mice

Li Ma[1,2], **Yinhui Zhou**[1], **Mohammed A. S. Khan**[1], **Shingo Yasuhara**[1], and **J. A. Jeevendra Martyn**[1]

[1]Department of Anesthesiology, Critical Care and Pain Medicine, Massachusetts General Hospital, Shriners Hospital for Children, Boston and Harvard Medical School, Boston, MA, USA

[2]Department of Burn & Plastic Surgery, First Hospital affiliated to General Hospital of the Chinese People's Liberation Army, Beijing, China

Abstract

Introduction: Burn injury (BI) leads to both systemic and neuro-inflammation and is associated with muscle wasting and weakness, which increase morbidity and mortality. Disuse atrophy is concomitantly present in BI patients. Most studies have focused on muscle with little attention to role of central nervous system (CNS) in the neuromuscular changes. We tested the hypothesis that BI-induced muscle wasting stems from CNS microglia activation and cytokines and chemokine release, that is associated with spinal ventral horn motor neuron degeneration.

Methods: Body surface (35%) BI, immobilization alone (Immob), BI with immobilization (BI +Immob) or Sham BI was administered to mice. Spinal cord (L3-L4 segments) and skeletal muscle tissues were harvested on day 7 and 14 after perturbations to examine microglia, motor neuron and skeletal muscle changes.

Results: BI and BI+Immob significantly ($p < 0.05$) activated microglia, evidenced by its increased density around motor neurons, upregulated neuroinflammation-marker, TSPO expression and inflammatory cytokines (IL-1β, TNF-α) and/or chemokines (CXCL2) expression at day 7 and 14. Ventral horn motor neurons apoptosis and down-regulation were observed at both periods after BI and was significantly magnified by concomitant BI+Immob. BI and more prominently BI+Immob disintegrated and fragmented the pretzel-shaped synapse and was associated with significantly decreased gastrocnemius, tibialis and soleus muscle masses.

Conclusion: BI induces microglia proliferation and activation (cytokine and chemokine release), degeneration of ventral horn motor neurons and muscle mass loss, all of which were accentuated by concomitant immobilization. The mechanisms connecting microglia activation and motor neuron degeneration to muscle mass loss require further delineation.

Keywords

Burns; immobilization; microglia; motor neuron; neuromuscular junction; synapse; muscle wasting

Corresponding author J. A. Jeevendra Martyn, M.D., F.R.C.A., F.C.C.M., Department of Anesthesiology, Massachusetts General Hospital, 51 Blossom Street, Room 206, Boston, MA 02114. Phone: 617 726 8807; Fax: 617 371 4821, JMARTYN@mgh.harvard.edu.

Introduction

Approximately 450,000 patients receive hospital and emergency room treatment for burn injury (BI) each year with ~ 30,000 hospital admission (1). BI is among the most devastating of all injuries because it leads to systemic and neuroinflammation that leads to multiple organ system dysfunction with increased morbidity and mortality (2). Due to improved and longer survival from better critical care management, almost all severely BI patients demonstrate skeletal muscle wasting and weakness, which can lead to respiratory failure requiring mechanical ventilation, difficulties in weaning off respirators, and even death (3–4). Despite pharmacological therapy (e.g., propranolol, oxandrolone) and aggressive rehabilitation, profound loss of skeletal muscle mass and weakness continues to be present even after discharge from hospital (5–6). To date, most studies have focused on study of muscle factors *per se* with very little attention to the role of central nervous system (CNS) or specifically the spinal cord in the muscle changes and neuromuscular dysfunction.

Vetrichevvel et al (7) found increased CNS-related morbidity (burn injury cohort had 2.20 times as many nervous system-related admissions and 3.25 times the number of days in hospital than the uninjured cohort after BI, which lasted many years after BI. Peripheral neuropathies together with changes in conduction velocities and muscle changes have been observed (8–11), but their relationship to CNS changes have not been queried. A rat study reported that a localized BI to hind paw induced apoptotic death of ventral horn motor neurons and Schwann cells in sciatic nerve 4 or 8 weeks later in association with muscle atrophy and weakness (12). However, there is a dearth of information on the effects body BI on CNS changes and their relationship to muscle changes.

Systemic inflammation is a characteristic of severe BI and has been shown to release various cytokines from the inflammatory macrophages (13–14). However, clinical and basic studies do support the notion of neuro-inflammation following body BI (15–16). Microglia are the resident macrophages of the CNS. Microglia, when activated due to injury or infection release inflammatory cytokines and chemokine. Studies on the effects of body BI on the spinal cord microglia, microglia activation status after body BI and their connection to muscle changes are non-existent. In contrast to the previous study which documented a localized BI causing apoptotic changes in ventral horn supplying the injured area (12), this study tested the hypothesis that body BI produces distant effects on spinal cord ventral horn motor neuron via activation of CNS microglia that leads to cytokine and chemokine release, which is associated with synaptic and muscle mass changes. The secondary hypothesis was that the concomitant presence of immobilization (disuse-atrophy) produces more aggravated changes in the spinal motor neuron.

Materials & Methods

Methods

C57BL6/J mice were used and purchased from The Jackson Laboratory (Bar Harbor, ME). RNeasy plus Universal kit was from Qiagen (Germantown, MD). High Capacity RNA-to-cDNA Kit, Platinum SYBR Green qPCR Super Mix, ViiA7 Real-Time PCR System, Pierce

660nm Protein Assay kit, NuPAGE LDS Sample Buffer, NuPAGE 4–12% Bis-Tris Gel and Alexa Fluor™ 568 Antibody and Alexa Fluor 488 Polyclonal Antibody were from Thermo Fisher Life Technologies (Grand Island, NY). ApopTag fluorescein kit S7110 for *in situ* apoptosis detection and primary antibody against NeuN (neuronal marker) were obtain from Millipore Sigma (Burlington, MA). Nova Ultra Nissl stain kit was from IHC world (Woodstock, MD). Primary antibody IBA1 (microglia marker) was obtained from FUJIFILM Wako Pure Chemical Corporation (Japan), primary antibody NeuN was obtained from Merck Millipore (Bedford, MA), primary antibody MuRF1 (muscle specific ubiquitin ligase) was obtained from Santa Cruz Biotechnology (Santa Cruz, CA), and primary antibody for TSPO (translocator protein 18 kDa, an inflammatory response marker in immune cells), TNF alpha, IL-1 beta were obtained from Cell Signaling Technology, Inc (Danvers, MA). Atrogin-1(muscle specific ubiquitin ligase) was from Abcam (Cambridge, MA). Alexa Flour 594-labeled α-Bungarotoxin for labeling of synaptic acetylcholine receptor was from Molecular Probe S (Carlsbad, CA). HRP-conjugated anti-rabbit IgG antibody was from EMD Millipore (Danvers, MA). Protease inhibitor Cocktail were obtained from Sigma (St. Louis, MO).

Animal experimental design

The study protocol was approved by the Institutional Animal Care Committee at Massachusetts General Hospital (Protocol # 2013N000193). Newly arrived adult male mice (20–25 g, body weight.) was acclimated to the new environment for 1 week before carrying out experimental procedures. Mice (n=80) were randomly divided into four groups: Sham BI (SB), immobilization alone (Immob), BI (third-degree burn injury with 35% total body surface area) alone and BI with immobilization by external plastic casting (BI+Immob). The spinal cord and skeletal muscle tissues were harvested on day 7 and 14 after the perturbations described above. The study flow-chart is shown in Figure 1.

Burn injury and immobilization

Burn injury alone or with immobilization was produced under general anesthesia using Ketamine (50 mg/kg, b.w., given i.p.) and Xylazine (5 mg/kg, b.w., given i.p.) mixture. Third degree BI was produced to achieve 35% of total body surface area (TBSA) injury, by immersing the back side and both flanks of body for 8s and abdomen for 5s in 80°C water, as previously described (17). Fluid resuscitation was performed by injecting 1 ml of normal saline. Butorphanol (2 mg/kg, s.c.) was provided with saline as analgesia before surgery and then twice a day for 3 days. A weight- and time- matched SB and Immob alone groups were treated in the same manner as the BI group, except that they were immersed in lukewarm water. Immobilization of hind limb was produced by the external plastic casing (EPC) to prevent movement of the left hind limb, as previously described (18). After recovery from anesthesia, the mice were returned to the individual cages. Food was provided as usual at the bottom of the cage. At day 7 and 14 after the perturbations, the animals were euthanized and muscle tissues (gastrocnemius, soleus and tibialis anterior) and spinal cord (L3-L4 segments) were harvested.

Immunofluorescent staining

Mice were euthanized with overdoes of ketamine and xylazine mixture and perfused with 40mL of heparinized saline and 4% paraformaldehyde in 0.1 mol/L PBS. The spinal cords were removed and post fixed overnight in 4% paraformaldehyde in 0.1 mol/L PBS at 4°C, subsequently transferred to 15% and 30% sucrose solution. Lumbar spinal cords L3-L4 segments were collected and embedded in an optimal cutting temperature (OCT) compound for frozen sections and cut into 10 or 30μm thick slices. The sections were incubated in 1% BSA solution for 1 hour at room temperature and then incubated overnight with ionized calcium-binding adapter molecule 1 (IBA1, a microglia marker,, 1:300; Wako, Japan) and NeuN primary antibody (neuron marker, 1:300; Merck Millipore, Bedford, MA) at 4°C for staining neurons. The sections were washed with PBS before being incubated with Alexa Fluor 568 antibody and Alexa Fluor 488 polyclonal antibody for 1 hour at room temperature. The nuclear-staining agent DAPI was added as well. After a final wash with PBS, the sections were mounted on glass slides, air dried, and covered. Images were recorded by Nikon Eclipse microscope E800 and ZEISS LSM800 Confocal microscope, IBA1 positive cell (activity microglia) was calculated and measured by Volocity 3D image analysis software.

Nissl staining

To observe the morphology and number of motor neurons, 10μm thickness frozen sections of lumbar L3-L4 spinal cord segments were dried at room temperature. Then, the slices were dehydrated through 100% alcohol, 95% alcohol and distilled water, and stained according to Nova Ultra Nissl stain kit manufacturer (Woodstock, MD). Subsequently, the slices were immersed in 95% ethyl alcohol for 5 minutes, dehydrated in 100% alcohol and cleared in xylene for 5 minutes. Spinal cord slices were mounted and observed under Nikon Eclipse E800 light microscope. The average quantities of Nissl bodies (neurons with a diameter ≥25 μm) were counted by randomly selecting five Nissl-stained sections at the same site from each animal.

Apoptosis testing

L3-L4 segments of lumbar spinal cords were collected and embedded in OCT compound for frozen sections and cut into 10μm thick slices. Apoptotic cell death was detected using the TUNEL assay according to the manufacturer instructions (Millipore, ApopTag fluorescein in situ apoptosis detection kit S7110). Sections were also incubated overnight with NeuN primary antibody (1:300; Merck Millipore, Bedford, MA) at 4°C. Subsequently, sections were washed and incubated with Alexa Fluor 488 polyclonal antibody for 1 hour at room temperature. Nuclear-staining agent DAPI was added and mounted on glass slides. Images were recorded by Nikon Eclipse E800 microscope and the TUNEL/NeuN positive cells were counted in 3 fields (20×) for each section.

Real-time Quantitative PCR (QPCR)

To determine if BI induced microglia activation with an inflammatory response occurs in spinal cord, real-time quantitative PCR was used to analyze mRNA expression for cytokines and chemokines in lumbar spinal cords. Total RNA was extracted using RNeasy plus

Universal kit (Qiagen, Germantown, MD) from mouse lumbar spinal cord ventral segment isolated freshly. cDNA synthesis was accomplished using High Capacity RNA-to-cDNA Kit (Thermo Fisher Life Technologies) followed by real-time PCR. Real-time RT-PCR reactions were carried out using Platinum SYBR Green qPCR Super Mix (Thermo Fisher Life Technologies) on a 7 ViiA7 Real-Time PCR System (Life Technologies). Primers used in this study are shown in Table 1. Each reaction was performed in triplicate independently with endogenous controls (mouse GAPDH) and experiments repeated.

Assessment of neuromuscular junction (NMJ) morphology

To observe the morphology of neuromuscular junction (synapse), gastrocnemius muscles were harvested. Frozen sections (30μm thickness) of gastrocnemius muscles were fixed in 4% paraformaldehyde followed by immunochemical staining with Alexa Flour 594-labeled α-Bungarotoxin (BTX Molecular Probes, Carlsbad, CA) as previously described protocol (18). BTX specifically binds to the acetylcholine receptors at the NMJ. After washing with PBS, the muscles were mounted on the slides. Digital images of NMJs from whole mount tissue preparations were obtained with a ZEISS LSM800 Confocal microscope.

Western blot

Spinal cord (L3-L4 segment) and gastrocnemius muscles were homogenized in tissue lysis buffer (Sigma, St. Louis, MO) containing complete protease inhibitor. After centrifugation of homogenates at 12,000g for 15 minutes at 4°C, the supernatants were collected. Protein concentrations were determined using the BCA protein assay (Pierce, Grand Island, NY). Equal protein amounts were separated by 4–12% Nu-PAGE and transferred onto polyvinylidene difluoride membranes. Then, the membranes were blocked in blocking buffer for 1 h. Spinal cord membranes were incubated with primary antibodies TSPO (1:10000, CST, Danvers, MA), TNF-α (1:1000, CST, Danvers, MA), IL-1β (1:1000, CST, Danvers, MA) and gastrocnemius muscle membranes were incubated with primary antibodies anti-atrogin-1 (1:500, Abcam, Cambridge, MA) and anti- MuRF1 (1:200, Santa Cruz, CA) overnight at 4°C. Atrogin-1and MuRF1 are proteolytic enzymes upregulated in muscle wasting conditions. After three washes, the membranes were incubated with HRP-conjugated anti-rabbit IgG antibody for 1 hour at room temperature. Immuno-reactive proteins were visualized by using a chemiluminescent detection kit and the detected bands were quantified by using the NIH Image J software, with protein expression levels expressed as the gray value ratio of target protein to GAPDH.

Statistical analysis

All data are expressed as the mean ± SE and were analyzed using the Graph Prism Program, Version 5.0 (Graph Pad Software, Inc., La Jolla, CA, USA). Comparisons differences between groups were performed using one-way ANOVA and subjected to Tukey's multiple comparison tests. A p-value < 0.05 was considered statistically significant.

Results

Burn injury induces microglia activation in ventral horn of spinal cord

First, the density and morphological phenotypes of microglia in ventral horn of spinal cord were investigated by immunofluorescent staining on sections of L3-L4 segments using ionized calcium-binding adapter molecule 1 (IBA1, a microglia marker). IBA1 positive cells were evaluated at days 7 and 14 after perturbations described previously. Compared to SB, significant increases of IBA1 positive cells (white arrows in Fig.2A) were observed in the ventral horn of spinal cord in BI and BI+Immob group at the day 7 and 14 days. The highest increase in IBA1 immuno-reactive cells was observed at 14 days in BI+ Immob group (white arrows in Fig.2A). The IBA1 positive cell in the Immob alone group was not significantly different compared to SB. The proliferated microglia in BI and BI+Immob group appeared to surround the motor neurons. To further understand the morphology and density change of microglia in ventral horn, magnified images of microglia were matched with NeuN staining of motor neurons nuclei in ventral horn. A dramatic increase of the microglia surrounding the neuron somata was observed in BI and particularly in BI+Immob group at day 14 (Fig. 2B).The morphology of microglia in the BI, BI+Immob groups exhibited hypertrophic and short, thick processes compared to sham which exhibited smaller thin processes. As described in the Methods section, we measured the increased in activity using Volocity 3D image analysis software. It was found that IBA1 activity of microglia cells increased at day 14 in BI and BI+Immob to 16.33±2.18, 18.33±3.33 per fraction area, respectively, compared 4.66±1.20 in SB group, $p<0.05$. The volume of body size increase in the BI and BI+Immob group to 316.2±27.44, 323.1±33.92 μm^3 at day 14, respectively compared SB group 186.8±11.55 μm^3, $p<0.05$ (Fig. 2C). The immobilization alone did not significantly affect the IBA1 expression (Fig. 2C).

Microglia activation was further confirmed by immunoblot analysis using TSPO expression. TSPO, the translocator protein 18 kDa, is dramatically upregulated in neuroinflammatory conditions, especially in activated microglial cells (19). Therefore, we examined the TSPO expression in ventral horn spinal cord. As shown in Fig. 3B, a significant increase of the TSPO/GAPDH ratio was observed at day 7 in the BI and BI+Immob group (3.1±0.41, 2.91±0.67 compared to SB 0.72±0.14, $p<0.05$). The TSPO expression was higher at day 14 in BI and BI+Immob group (4.78±0.58, 5.69±0.82 compared to 0.63±0.37, $p<0.05$). Immobilization alone, however, did not significantly induce the TSPO expression in microglia (Fig. 3B).

Burn induced pro-inflammatory cytokines and chemokines expression

Previous studies in other pathological stated have demonstrated that microglia activation leads to pro-inflammatory cytokine release (20). We, therefore, examined if body BI leads to pro-inflammatory cytokines and chemokines expression at a site distant from BI, the spinal cord. The L3-L4 spinal cord segments, a region not innervating BI area (back side, flank and abdomen) were collected at day 7 and 14 post BI, BI+Immob, Immob alone or SB. The transcriptional expression of cytokines (including IL-1β, IL-6, IL-10 and TNF-α) and chemokines (CXCL2 and MCP-1) were examined by RT-PCR. The mRNA levels of pro-inflammatory IL-1β, TNF-α, CXCL2 and MCP-1(a.k.a., CCR2) in BI group were up-

regulated to 4.7, 3.3, 20.0, 1.4 fold at 7 days, respectively. The expression of IL-1β, TNF-α, CXCL2 and MCP-1 was upregulated to 16.5, 11.8, 8.4, 3.0 fold at 14 days respectively, compared to SB group (p<0.05, Fig.3A). In BI+Immob group the expression of IL-1β, TNF-α and CXCL2 mRNA significantly increased 10.3, 4.0, 7.9 fold at 14 days (p<0.05, Fig.3A), respectively. The mRNA levels of anti-inflammatory, IL-10 also significantly increased in BI and BI+Immob group compared with SB 1.9, 1.3 at 7days and 1.8 and2.6 fold at 14 days). However, IL-6 mRNA levels did not differ between groups (p>0.05), expect in BI+Immob at day 14 *vs.* SB (p<0.05, Fig.3A).

In view of the presence of inflammatory proteins in the BI with or without immobilization, the protein expression of IL-1β and TNF-α were also assessed by immunoblot analyses of ventral horn spinal cord. The immunoblots showed increased expression of IL-1β in BI and BI+Immob group (1.96±0.31, 2.48±0.18 fold, respectively, compared to SB 0.63±0.24 at 7days and 1.92±0.27 and 2.11±0.18 fold, respectively, compared to SB 0.73±0.17 at 14 days, Fig 3C). Clearly, the increase of TNF-α/GAPDH ratio was significantly induced by BI with or without immobilization treatment to (1.11±0.11, 1.32±0.27 vs. 0.09±0.08 at day 7 and 1.68±0.18, 1.19±0.32 vs. 0.049±0.17 at day 14, Fig. 3C). Thus, these findings strongly support the role of BI, particularly with immobilization to induce pro-inflammatory cytokines expression in the spinal cord.

Burn Injury decreased Ventral Horn Motor Neurons

We next examined the change of motor neurons in ventral horn spinal cord induced by BI at day 14 after injury. The lumbar spinal cord segments were harvested and evaluated by Nissl Stain and immune-fluorescence staining. In the SB group, the ventral horn had large amount of Nissl stained bodies in the cytoplasm and the nuclei were lightly stained with a clearly visible nucleolus (Fig.4A). Compared with SB, there were fewer morphologically normal neurons after BI, and cells appeared swollen with a darkly stained and shrunken cytoplasm. Vacuolation with pyknosis was observed and Nissl bodies decreased especially in BI +Immob group (Fig.4A). As in previous studies, ventral horn with a diameter of ≥25 μm were counted as motor neurons in spinal cord. Using this criterion, we counted the motor neurons in ventral horn of spinal cord and found that morphologically normal motor neurons decreased after BI and BI with immobilization at 14 days, especially on the immobilization side of BI+Immob group (Fig. 4B) (7.34±3.54 compared SB value of 15.95±4.34, p<0.05). The motor neuron numbers were not affected in the immobilization alone group (Fig. 4B) (14.57±4.87 compared SB value of 15.95±4.34, p>0.05). Thus BI plus immobilization had the greatest effect on microglia activation and motor neuron decrease, while immobilization alone did not affect motor neuron number.

Burn increases apoptotic cells in Lumbar Ventral Horn Motor Neurons

Next, the apoptotic cells in the ventral horn at L3-L4 segments were re-evaluated by TUNEL assay. No apoptotic cells were observed in the SB and Immob group. In BI group, few TUNEL/NeuN positive cells were scattered in ventral horns spinal cord tissue at day 7 (Image didn't shown). However, TUNEL/NeuN positive apoptotic cells were observed at days 14 in BI and BI+Immob group (p < 0.05, Fig.4C).

Muscle wasting following burn injury

We next examined the muscle mass changes following BI. Muscle mass changes in gastrocnemius, tibialis anterior and soleus muscles at day 14 were measured by the dry muscle weight/preburn body weight) ratio (Fig. 5A). Compared with SB group, the gastrocnemius, tibialis anterior and soleus muscles masses were decreased ~19– 38% in Immob, BI, and BI+Immob group (Fig. 5A). Moreover, we found that the reduction in skeletal muscle was greatest in BI+Immob group at day14 ($p<0.05$). We next examined the muscle atrophy marker MuRF-1 and atrogin-1 by western blots of gastrocnemius muscles at day 14 after injury. As showed in Figure 5B, MuRF-1 was significantly increased at day 14 in the Immob alone, BI and BI+Immob groups. The atrogin-1 protein was also upregulated in the 3 experimental groups. There was no significant difference in the expression of the proteolytic enzymes between Immob, BI and BI+Immob group at day 14 ($p>0.05$). These results suggest that skeletal muscle proteolytic pathways were activated in the response not only BI but also in immobilization at day 14.

Burn caused neuromuscular junction (NMJ) disintegration

To further explore if the neuromuscular synapse was disrupted by BI, which could add to the BI-induced neuromuscular dysfunction, the morphology of NMJ (synapse) was assessed. In SB, the NMJ in gastrocnemius muscle showed the typical pretzel-like shaped continuous aggregates of acetylcholine receptors (labeled by α-bungarotoxin). At day 14 after injury, the gastrocnemius muscle of Immob group did not reveal any specific alterations, while BI and BI+Immob group showed disintegrated and fragmented synapses (Fig.5C). The typical pretzel shape was lost and synapse was smaller and irregular in BI and BI+Immob group. These changes in morphology indicated that BI caused disruption of the NMJ or synapse.

Discussion

That the pathophysiological responses of severe BI leads to acute neuromuscular dysfunction; the prolonged neuromuscular dysfunction and disability subsequent to BI is also well established (21–22). However, the role of spinal cord changes in the neuromuscular changes after BI are uncharacterized. The present study provides a new insight into the distant effects of body BI on CNS spinal cord changes and their relationship to synaptic and muscle changes. In this study, we demonstrate that a 35% body area third degree body BI induces activation of microglia and degeneration of spinal cord ventral horn neurons, which is associated with synaptic degeneration and muscle atrophy. The microglial activation was evidenced by both morphologically (proliferation of numbers demonstrated by IBA1 staining) and biochemically (increased expression of activated microglial cell marker TSPO, cytokines and chemokines). Neuronal cells do not release cytokines (23). The spinal cord and neuromuscular changes of BI seem to be exaggerated by the concomitant presence of immobilization of the limb.

Microglia are the resident macrophages of the CNS and play an important role in rapidly responding many forms of stimuli including injury and infection (24–25). It is possible that damage-associated molecular patterns (DAMPS) released from BI sites permeate the blood-brain barrier and cause the microglia activation. Among spinal cord tissues, the IBA1

antibody specifically binds to microglia (26). Thus, this study used IBA1 for assessment of microglia proliferation (activation). At 7 and 14 days after the injury, the density of IBA1 positive cells significantly increased in ventral horn of spinal cord of BI animals with or without immobilization. The largest numbers of IBA1 positive cells were observed at day 14 in BI+ Immob group, when compared with SB. TSPO expression in microglia is the now commonly used to image neuroinflammation as its expression is upregulated in reactive microglial cells during CNS pathologies. Our study, in addition to IBA1 expression, confirmed microglia activation evidenced by the higher TSPO expression in BI and BI +Immob group. There is *a priori* evidence (27–28) that resident microglia, when activated release inflammatory cytokines and chemokines. Although the initial release of these inflammatory mediators is a protective response to a change its microenvironment against organisms, its continued activation can cause deleterious effects because of the persistent presence of these inflammatory mediators.

An obvious change in morphological phenotype was observed after BI-induced microglia activation. At 14 days after BI, the slender microglia phenotype disappeared and most of the proliferated microglia exhibited hypertrophic and short, thick processes with extensive overlap; in other words, the morphology of microglia in spinal cord changed from ramified to amoeboid type, and the body size also increased which are the classic morphologic appearance of the activated microglia phenotype. *Parri passu* with the altered phenotype, BI significantly increased spinal cord levels of the inflammatory cytokines IL-1β and TNFα mRNA and protein expression at day 7 and 14. However, the pro-inflammatory cytokines IL-6 mRNA was unaltered, except in the BI+Immob-14d group. It is possible that IL-6 levels increased and decreased at an earlier period than was examined in this study. A transient rise of IL-6 after BI has been previously reported (29–30). Increased mRNA levels of anti-inflammatory IL-10 was also noted in BI and BI+Immob group at 14 days, which most likely is a response to the increase in the inflammatory mediators to counteract the inflammatory responses.

Recent studies (31) implicated that several chemokines are increased in the spinal cord after peripheral nerve injury that attract leukocytes to the injury site. In the current study, a rise in levels of the chemokines CXCL2 and MCP-1 mRNA expression were detected, especially at 7 days after injury, which persisted to 14 days post injury. These changes are consistent with the notion that BI is associated with a neuro-inflammatory response. CXCL2, is upregulated and released by spinal glia cells during inflammation and contributes to the pathogenesis of inflammatory diseases. MCP-1 is another important chemokines, plays a critical role in the migration of bone marrow-derived and resident monocyte cells to sites of inflammation. The BI-induced microglial activation and the secretion of CXCL2 and MCP-1 and migration of non-neuronal cells may have contributed to the development of neuro-inflammation and neuro-degeneration (loss of ventral horn motor neuron by apoptosis).

Wu *et al* (12) have reported that local hind paw burn induces apoptosis in spinal cord ventral horn motor neurons and Schwann cells in sciatic nerve 4 or 8 weeks after injury. Microglia activation have been implicated as a trigger factor of motor neuron death. Several studies document microglia cells gathering on nerve injured sites in spinal cord after trauma or other injuries (27–28, 32), and abundance of the inflammatory cytokines and chemokines

contributed to neuron death/degeneration or acute peripheral motor neuropathy (31–34). The detrimental effects of chemokines and cytokines on motor neuron damage has also been well exemplified in other non-traumatic acquired pathologic states such multiple sclerosis and amyotrophic lateral sclerosis (27–28). Consistently, we also note a greater accumulation of activated microglia around the microenvironment of apoptotic neurons after BI, and BI +Immob. Furthermore, we observed that motor neuron cells of L3-L4 ventral horn spinal cord during Nissl staining the BI group neuronal cells appeared swollen with dark Nissl staining, shrunken cytoplasm and Nissl bodies decreased. Most notably the vacuolation, pyknosis and Nissl bodies decrease were worse in BI+Immob group. The motor neurons degeneration evidenced by these studies may due to the apoptotic cell death of the spinal cord ventral horn effected by activated microglia. An alternative explanation, which requires further study is whether the proliferation and migration of microglia towards the motor neuron area occurs in order to phagocytose the apoptotic neurons.

The main function of ventral horn motor neurons is transmission of impulses from the motor neuron to the synapse (NMJ) to release acetylcholine and generate force in muscle. Loss of motor neurons function due to its decrease in number from apoptotic death can lead to ineffective neurotransmission via synapse muscle weakness and wasting (atrophy) of muscle as demonstrated in many neurological diseases affecting motor neuron (e.g., amyotrophic lateral sclerosis and multiple sclerosis (14,27–28)). In the current study, we note change of skeletal muscle mass with BI in association with the motor neuron changes. The gastrocnemius and soleus muscles masses were decreased progressively with time in BI and BI+Immob group. There was a 45% loss in soleus muscle mass and a 25% decrease in gastrocnemius by 14 days after BI with or without immobilization. Meanwhile, using western blot we found the expression of muscle specific ubiquitin ligases MuRF-1 and atrogin-1 highly expressed in BI and BI+Immob group. We also found in SB group, gastrocnemius muscle showed the normal pretzel-like shaped NMJ morphology, whereas muscle of BI and BI+ Immob group mice showed obvious morphological alterations-markedly fragmented synapse at 7, 14 days after injury. Both the motor neuron and skeletal muscle transmit signals to each other to maintain their mutual integrity (35). Synaptic integrity, however, is pivotal for this communication between the motor neuron and myofiber. Active muscle contraction is required for the retrograde signals from muscle to nerve (35). The worsening of the motor neuron denervation with immobilization may be related to the lack of muscle to nerve retrograde signals in the presence of immobilization. Thus, our observation of a more severe apoptosis and motor neuron down-regulation with BI +Immob vs. BI alone.

We note that immobilization alone also shows a significant muscle loss and upregulation of MuRF-1 and atrogin-1 proteins, without obvious microglia activation, motor neurons degeneration or neuromuscular junction change. In contrast, BI with concomitant presence of immobilization produced more aggravated changes in the spinal motor neuron, synaptic instability and muscle wasting. Thus for a role in spinal ventral horn changes BI with its associated with microglia activation and cytokine release seems to be essential for the motor neuron changes to occur.

Conclusion

The current study demonstrates that severe BI is sufficient to induce activation of microglia with release of inflammatory cytokine and chemokine release and degeneration of motor neurons in spinal cord ventral horn, which causes corresponding changes in the synapse and muscle mass loss (Fig. 6). The concomitant presence of immobilization with BI aggravates the muscle mass loss. The underlying mechanisms of the connection between microglia activation and motor neuron loss, and the effects of modulation of microglia activation by therapeutic maneuvers to reduce motor neuron and muscle mass loss requires further study.

Acknowledgements:

Supported in part by grants from Shriners Hospital for Children (#86300), Tampa, FL and from the NIH, P-50 GM2500 Project 1 and R01 GM 11847 (to JAJM).

Reference

1. Burn Incidence and Treatment in the United States: 2016 Fact Sheet. Chicago, IL: American Burn Association; 2012.
2. Nguyen L N, Nguyen T G: Characteristics and outcomes of multiple organ dysfunction syndrome among severe-burn patients. Burns 35(7):937–941, 2009. [PubMed: 19553020]
3. Hart DW, Wolf SE, Mlcak R, Chinkes DL, Ramzy PI, Obeng MK, Ferrando AA, Wolfe RR, Herndon DN:: Persistence of muscle catabolism after severe burn. Surgery 128(2):312, 2000. [PubMed: 10923010]
4. Porter C, Hurren NM, Herndon DN, Borsheim E: Whole body and skeletal muscle protein turnover in recovery from burns. International journal of burns and trauma 3(3):9–17, 2013. [PubMed: 23386981]
5. Porter C, Tompkins RG, Finnerty CC, Sidossis LS, Suman OE, Herndon DN: The metabolic stress response to burn trauma: current understanding and therapies. Lancet 388(10052):1417–1426, 2016. [PubMed: 27707498]
6. Clark Audra, Imran Jonathan, Madni Tarik, Steven E Wolf: Nutrition and metabolism in burn patients. Burns & Trauma 5(1):11, 2017. [PubMed: 28428966]
7. Vetrichevvel Thirthar P, Randal Sean M, Fear Mark W, Wood Fiona M, Boyd James H, Duke Janine M: Burn injury and long-term nervous system morbidity: a population-based cohort study. Bmj Open 6(9):e012668, 2016.
8. Tu Y, Lineaweaver WC, Zheng X, Chen Z, Mullins F, Zhang F: Burn-related peripheral neuropathy: A systematic review. Burns Journal of the International Society for Burn Injuries 43(4):693, 2017. [PubMed: 28347546]
9. Tamam Y, Tamam C, Tamam B, Ustundag M, Orak M, Tasdemir N: Peripheral neuropathy after burn injury. European Review for Medical & Pharmacological Sciences 17 Suppl 1(supplement 1): 107–111, 2013. [PubMed: 23436672]
10. Strong AL, Agarwal S, Cederna PS, Levi B: Peripheral neuropathy and nerve compression syndromes lead to substantial morbidity following burn injury. Clin Plast Surg 44(4):793–803, 2017. [PubMed: 28888304]
11. Higashimori H, Whetzel TP, Mahmood T, Carlsen RC: Peripheral axon caliber and conduction velocity are decreased after burn injury in mice. Muscle & Nerve 31(5):610–620, 2005. [PubMed: 15779020]
12. Wu SH, Huang SH, Cheng KI, Chai CY, Yeh JL, Wu TC, Hsu YC, Kwan AL: Third-Degree Hindpaw Burn Injury Induced Apoptosis of Lumbar Spinal Cord Ventral Horn Motor Neurons and Sciatic Nerve and Muscle Atrophy in Rats. Biomed Research International 2015(2):372819, 2015. [PubMed: 25695065]

13. Lavrentieva A, Kontakiotis T, Lazaridis L, Tsotsolis N, Koumis J, Kyriazis G, Bitzani M:Inflammatory markers in patients with severe burn injury. What is the best indicator of sepsis? Burns 33(2):189–194, 2007. [PubMed: 17215085]
14. Korkmaz HI, Krijnen PAJ, Ulrich MMW, de Jong E, van Zuijlen PPM, Niessen HWM: The role of complement in the acute phase response after burns. Burns Journal of the International Society for Burn Injuries 43(7), 2017.
15. Gatson JW, Liu MM, Rivera-Chavez FA, Minei JP, Wolf SE: Serum Levels of Neurofilament-H are Elevated in Patients Suffering From Severe Burns. Journal of Burn Care & Research 36(5):545, 2016.
16. Gatson JW, Liu MM, Rivera-Chavez FA, Minei JP, Wolf SE: Estrogen treatment following severe burn injury reduces brain inflammation and apoptotic signaling. Journal of Neuroinflammation 6(1):30, 2009. [PubMed: 19849845]
17. Hosokawa S, Koseki H, Nagashima M, Maeyama Y, Yomogida K, Mehr C, Rutledge M, Greenfeld H, Kaneki M, Tompkins RG, et al.: Title efficacy of phosphodiesterase 5 inhibitor on distant burn-induced muscle autophagy, microcirculation, and survival rate. Am J Physiol Endocrinol Metab 304(9):E922–E933, 2013. [PubMed: 23512808]
18. Khan MA, Sahani N, Neville KA, Nagashima M, Lee S, Sasakawa T, Kaneki M, Martyn JA: Nonsurgically induced disuse muscle atrophy and neuromuscular dysfunction upregulates alpha7 acetylcholine receptors. Canadian Journal of Physiology & Pharmacology 92(1):1–8, 2014. [PubMed: 24383867]
19. Karlstetter M, Nothdurfter C, Aslanidis A, Moeller K, Horn F, Scholz R, Neumann H, Weber BH, Rupprecht R, Langmann T: Translocator protein (18 kDa) (TSPO) is expressed in reactive retinal microglia and modulates microglial inflammation and phagocytosis. Journal of Neuroinflammation 11(1):3–3, 2014. [PubMed: 24397957]
20. Smith JA, Das A, Ray SK, Banik NL: Role of pro-inflammatory cytokines released from microglia in neurodegenerative diseases. Brain Research Bulletin 87(1):10–20, 2012. [PubMed: 22024597]
21. Tomera JF, Martyn J, Hoaglin DC: Neuromuscular dysfunction in burns and its relationship to burn size, hypermetabolism, and immunosuppression. Journal of Trauma & Acute Care Surgery 28(10): 1499–504, 1988.
22. Herndon David N. (Ed.): Total Burn Care 4th Edition. 6 2012, USA, Elsevier Saunders, pp395.
23. Hutchinson MR, Shavit Y, Grace PM, Rice KC, Maier SF, Watkins LR: Exploring the neuroimmunopharmacology of opioids: an integrative review of mechanisms of central immune signaling and their implications for opioid analgesia. Pharmacol Rev 63:772–810, 2011. [PubMed: 21752874]
24. Orr MB, Gensel JC: Spinal Cord Injury Scarring and Inflammation: Therapies Targeting Glial and Inflammatory Responses. Neurotherapeutics. doi: 10.1007/s13311-018-0631-6, 2018.
25. Pósfai B, Cserép C, Orsolits B, Dénes Á: New insights into microglia-neuron interactions: a neuron's perspective. Neuroscience pii: S0306–4522(18)30320–8, 2018.
26. Imai Y, Kohsaka S: Intracellular signaling in MCSFinduced microglia activation: Role of Iba1. Glia 40(2):164–1742002.
27. Cheng W, Chen G: Chemokines and Chemokine Receptors in Multiple Sclerosis. Mediators of Inflammation (8):659206, 2014. [PubMed: 24639600]
28. Philips T, Robberecht W: Neuroinflammation in amyotrophic lateral sclerosis: role of glial activation in motor neuron disease. Lancet Neurology 10(3):253–263, 2011. [PubMed: 21349440]
29. Kim HS, Kim JH, Yim H, Kim D: Changes in the Levels of Interleukins 6, 8, and 10, Tumor Necrosis Factor Alpha, and Granulocyte-colony Stimulating Factor in Korean Burn Patients: Relation to Burn Size and Postburn Time. Annals of Laboratory Medicine 32(5):339, 2012. [PubMed: 22950069]
30. Finnerty CC, Przkora R, Herndon DN, et al.: Cytokine expression profile over time in burned mice. Cytokine 45(1):20–25, 2009. [PubMed: 19019696]
31. Ramesh G, Maclean AG, Philipp MT. Cytokines and Chemokines at the Crossroads of Neuroinflammation, Neurodegeneration, and Neuropathic Pain. Mediators of Inflammation (9): 480739, 2013. [PubMed: 23997430]

32. Finnerty CC, Przkora R, Herndon DN, Jeschke MG: The role of inflammatory processes in Alzheimer's disease. Inflammopharmacology 20(3):109–126, 2012. [PubMed: 22535513]

33. Suzumura A: Neuron-microglia interaction in neuroinflammation. Current Protein & Peptide Science 14(1):16, 2013. [PubMed: 23544747]

34. Skaper SS, Facci L, Zusso M, Giusti P: An inflammation-centric view of neurological disease: beyond the neuron. Front Cell Neurosci. doi: 10.3389/fncel.2018.00072. eCollection, 2018.

35. Vilmont V, Cadot B, Ouanounou G, Gomes ER: A system for studying mechanisms of neuromuscular junction development and maintenance. Development 143(13):2464–2477, 2016. [PubMed: 27226316]

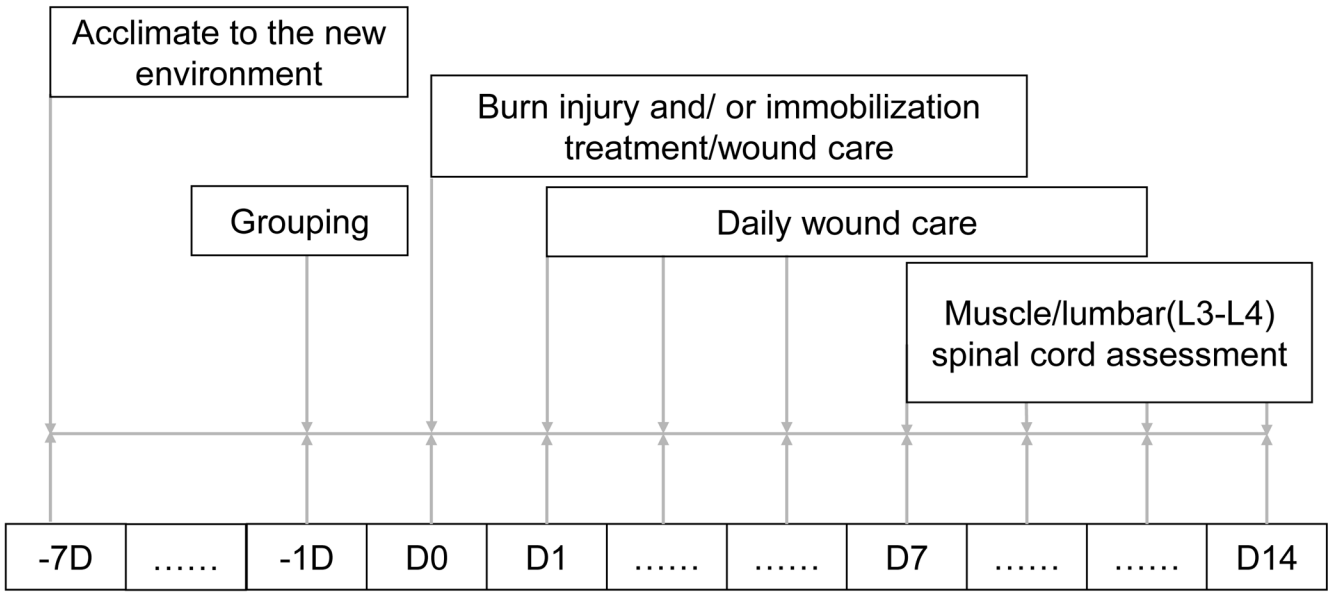

Fig. 1. Flow chart of the study.

D indicates day. Animals were purchased at least one week before start experiments (−7D). One day (−1D) before burn injury, mice were designed to four groups: sham burn (SB) and sham burn with immobilization (Immob), burn injury (BI) alone, BI with immobilization (BI +Immob). D0 refers to day of SB, Immob, BI and BI+Immob treatment. Daily wound care was provided by application 1% silver sulfadiazine cream. At 7 or 14 days after perturbations, spinal cord (L3-L4 segment) and gastrocnemius, tibialis anterior and soleus muscle were harvested.

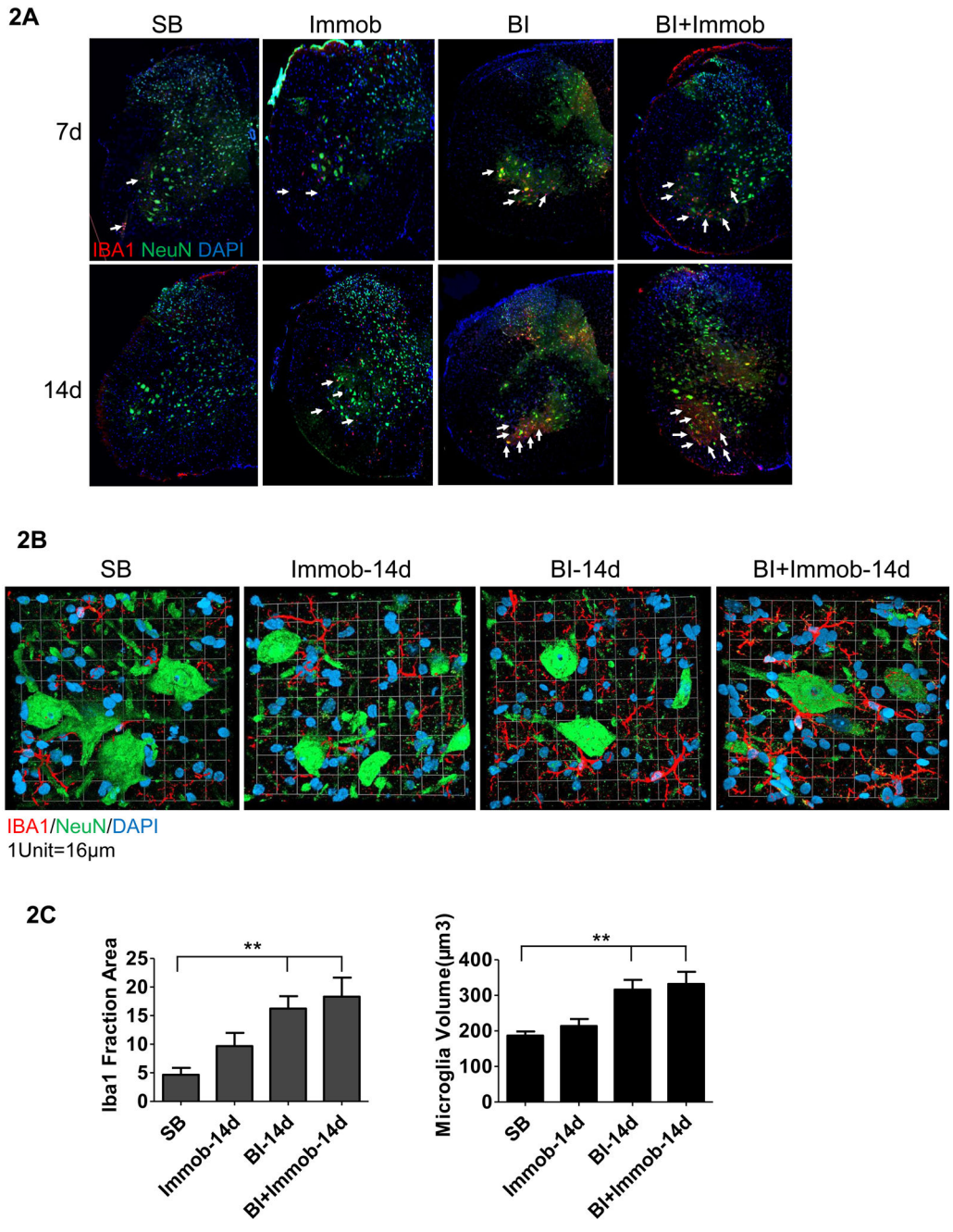

Fig. 2. Activation of microglia in spinal cord ventral horn after distant body burn injury.

(A) Confocal images of triple immunofluorescence staining of spinal cord ventral horn with microglia marker IBA1 (red color, white arrows pointed to), neuron marker, NeuN (green color) and nucleus (DAPI, blue) at 7 or 14 days post perturbations. Microglia proliferation was most visible in BI and BI with immobilization at day 14. (B) Figure demonstrates magnified images (magnification 63×) of the spinal cord ventral horn microglia and motor neuron in SB, Immob, BI and BI+Immob at day 14.n. The morphology of microglia exhibited hypertrophic and short, thick processes with extensive overlap in BI and BI +Immob groups; numerous microglia appeared to surround motor neurons. (C) Analysis on

the number and volume of microglia were performed on the fraction area of the ventral horn spinal cord section using Volocity 3D image analysis software, 5 sections /mouse, 4-6 animals/group. $^{**}p < 0.05$ vs. SB group. Microglia fraction and volume did not differ between SB and Immob. Both IBA1 fraction and volume of the microglia were significantly increased in BI and BI+Immob.

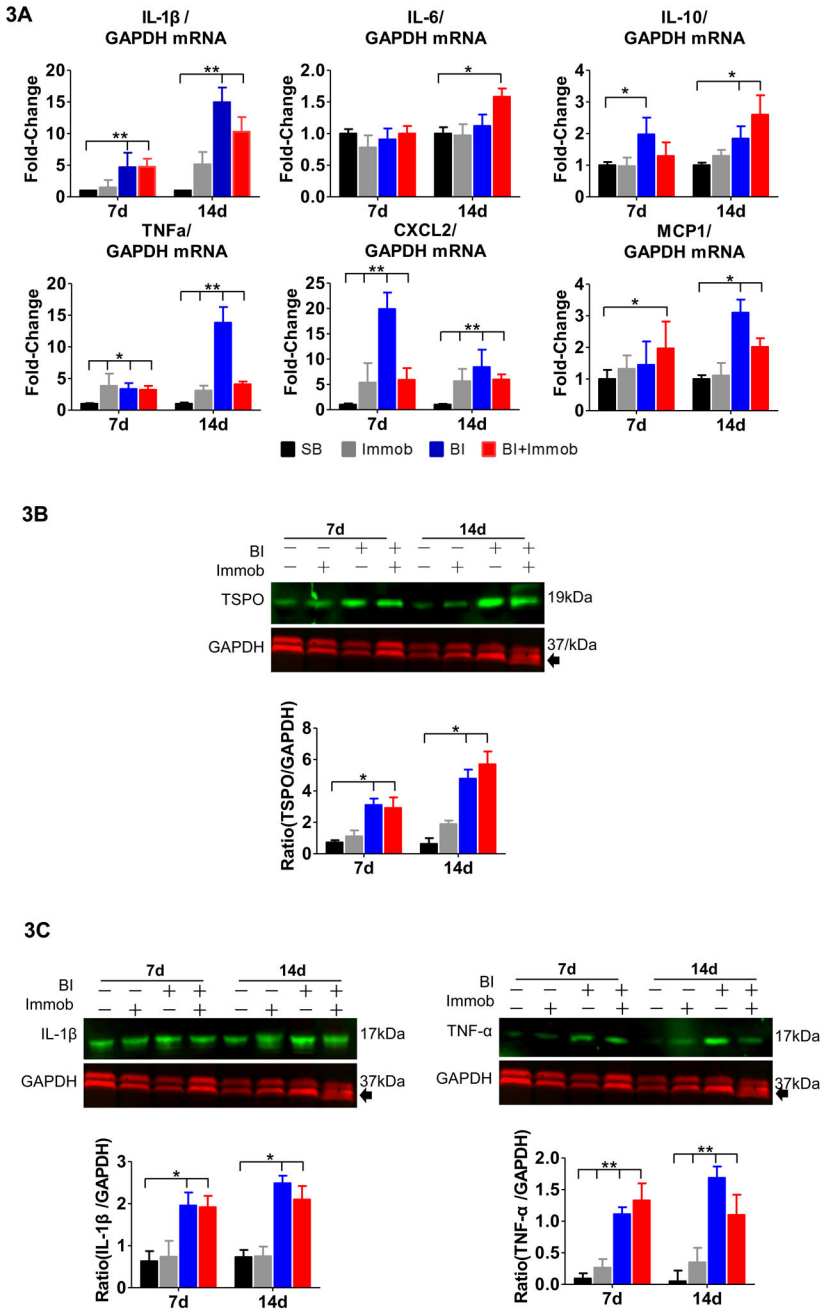

Fig. 3. Pro-inflammatory cytokines and chemokines expression in spinal cord after distant body burn injury.

(A) Quantitative PCR mRNA expression of cytokines (IL-1β, IL-6, IL-10 and TNFα) and chemokines (CXCL2 and MCP1) were measured and normalized to GAPDH. The mRNA expression of pro-inflammatory and chemokine molecules, IL-1β, TNF-α, and CXCL2, MCP-1, was sharply increased at day 7 and/or 14 post-injury in BI or BI+Immob groups relative to SB. The mRNA expression of TNF-α and CXCL2 was significantly increased in Immob alone group compared to SB. (B) Immunoblots of lumbar spinal cord (L3-L4 segments) isolated from SB, Immob, BI and BI+Immob mice at day 7 and 14 post-injury

probed for TSPO and normalized to GAPDH as loading control and fold change of the immunoblot was determined using Image J to measure band intensities of target protein to GAPDH. The expression of TSPO, a marker of microglial activation, was significantly upregulated in BI and BI+Immob at both 7 and 14 days post perturbation. (C) Immunoblot of lumbar spinal cord (L3-L4 segment) protein isolated from SB, Immob, BI and BI+Immob mice at day 7 and 14 post-injury probed for IL-1β, TNF-α and normalized to GAPDH using Image J to measure band intensities of target proteins. The immunoblots confirm microglia activation and pro-inflammatory cytokine (IL-1β, TNF-α) release.to GAPDH (loading control). Data are means ± SE; SB: n = 6, Immob-7d: n=5, BI-7d: n = 6, BI+Immob-7d: n = 6, Immob-14d: n=5, BI-14d: n = 5, BI+Immob-14d: n = 6. *$p < 0.05$ for BI or BI+Immob vs. SB, **$p < 0.001$ for BI or BI+Immob vs. SB.

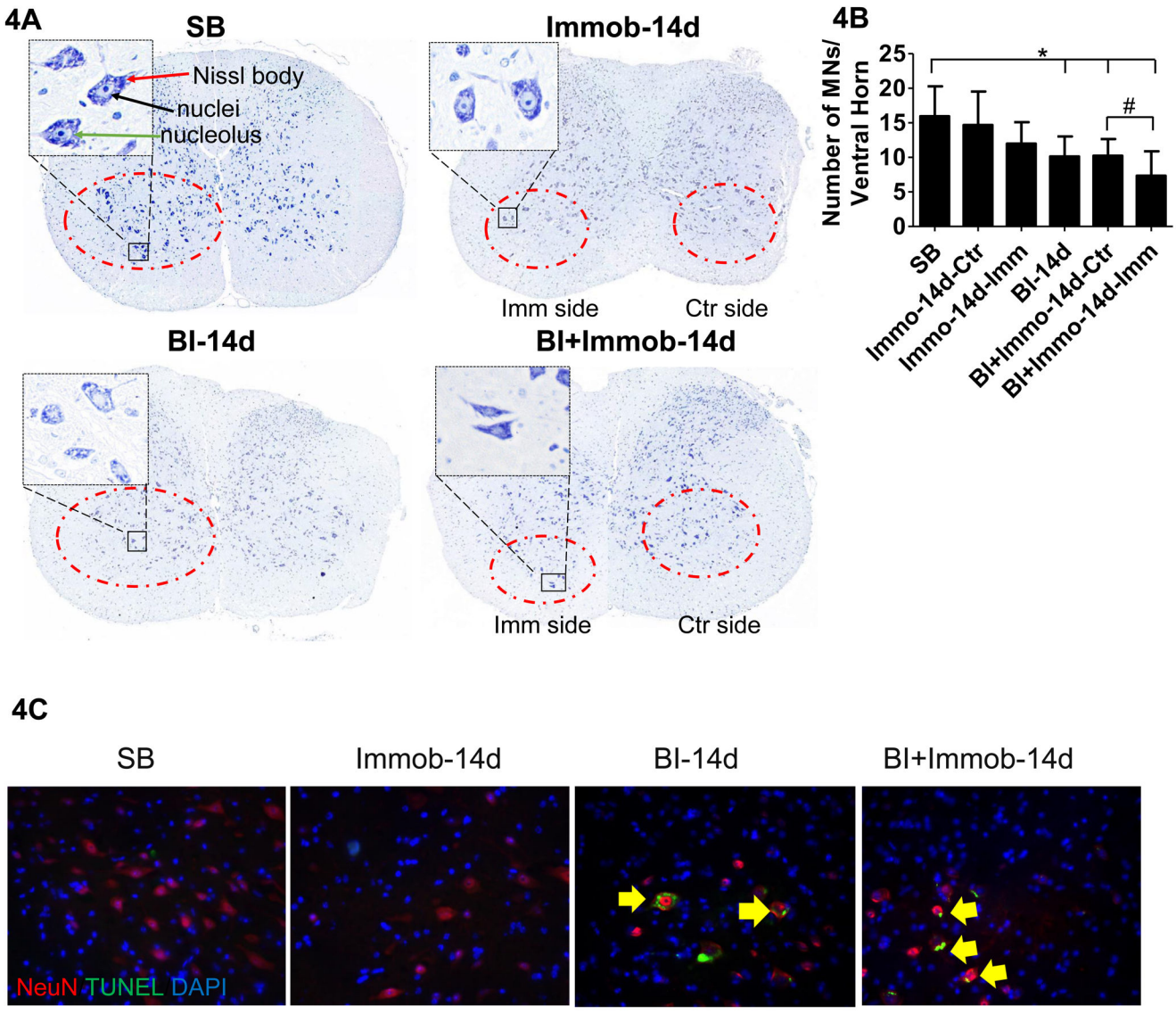

Fig. 4. Burn injury-induced apoptosis with decrease ventral horn motor neurons.

(A) Nissl staining of spinal cord dorsal and ventral horn. Imm side refers to immobilized side and Ctr refers to non-immobilized side of same animal. Compared to SB which show many Nissl stained bodies in the ventral horn, the BI group and BI+Immob groups showed decreased Nissl staining at day 14. As same as SB group, Immob group motor neurons showed regular shape, clear nucleus and Nissl bodies in the cytoplasm. The ventral horn image is magnified (400X) on the left dorsum of figure. The magnified images show motor neurons in SB, Immob, BI and BI+Immob groups at day14 after perturbations. The Nissl body is indicated by red line, the nuclei by black line and, the nucleolus by green line. The cytoplasm with a clearly visible nuclei and nucleolus is seen in SB. In contrast, fewer morphologically normal neurons were visible in BI and BI+Immob group, especially in BI +Immob group Imm side. Motor neurons cells were swollen with shrunken cytoplasm or vacuolation; pyknosis was also observed in BI-14d and BI+Immob-14d groups. (B) Ventral horn motor neurons (diameter ≥25 μm) counts in spinal cord, indicate that morphologically

normal motor neurons decreased after BI and BI with immobilization. Data are means ± SE; SB: n = 12, Immob-14d: n = 10, BI-14d: n = 10, BI+Immob-14d: n = 12. *$p < 0.05$ for BI or BI+Immob vs. SB, #$p < 0.05$ for BI+Immob Imm side vs. BI+Immob Ctr side. (C) Double immunofluorescence staining and TUNEL staining for ventral horn motor neuron in spinal cord. The images show that BI and BI+Immob increased apoptotic cells in ventral horn motor neurons. Magnification 20×, red: motor neuron, green: TUNEL signal, blue: nucleus, yellow arrow indicates apoptotic motor neurons.

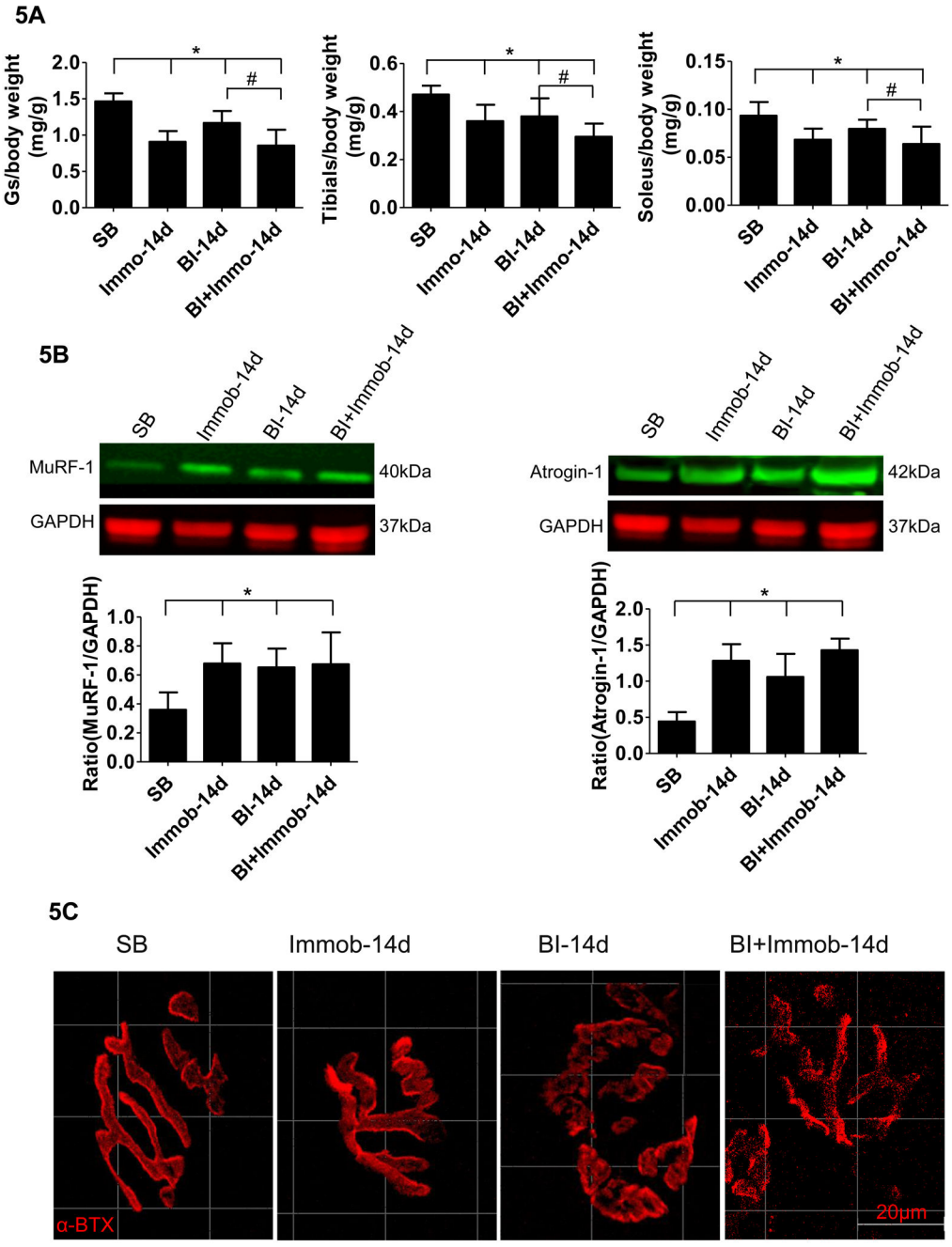

Fig. 5. Burn injury induced muscle wasting and neuromuscular junction synapse disintegration.

(A) The changes in muscle weight of SB, Immob, BI and BI+Immob group mice at day 14 post-injury. Dry muscle mass (gastrocnemius (Gs), soleus and tibialis anterior muscle) is expressed as a ratio to body weight at day preborn Day. The body weight ad day 0 was used in view of body weight loss induced by BI at day 14. Those histograms show that gastrocnemius, tibialis anterior and soleus muscles masses were decreased ~19- 38% at 14 days in Immob, BI, and BI+Immob group. Data are means ± SE; n = 5–8 mice/group. *p < 0.05 for Immob, BI or BI+ Immob vs. SB, #p<0.05 for BI+Immob vs.BI. (B) Immunoblots of muscle specific ubiquitin ligases, MuRF-1 and atrogin-1 expression in gastrocnemius

muscle, and quantitation of MuRF-1 and atrogin-1 expression normalized to GAPDH is shown. Those histograms show that MuRF-1 and atrogin-1 expression was significantly increased in the Immob, BI and BI+Immob groups. Data are means ± SE; n = 4 mice/group. *$p < 0.05$ for Immob, BI or BI+ Immob vs. SB; (C) Gastrocnemius muscles were stained with α-BTX (red color) to detect acetylcholine receptors at the muscle endplates (synapse). The endplate in SB and Immob group appear compact and pretzel shaped. In BI and BI +Immob group the synapses were fragmented, more marked in the latter group, evidenced by the loss of typical pretzel shape. Scale bar = 20 microns.

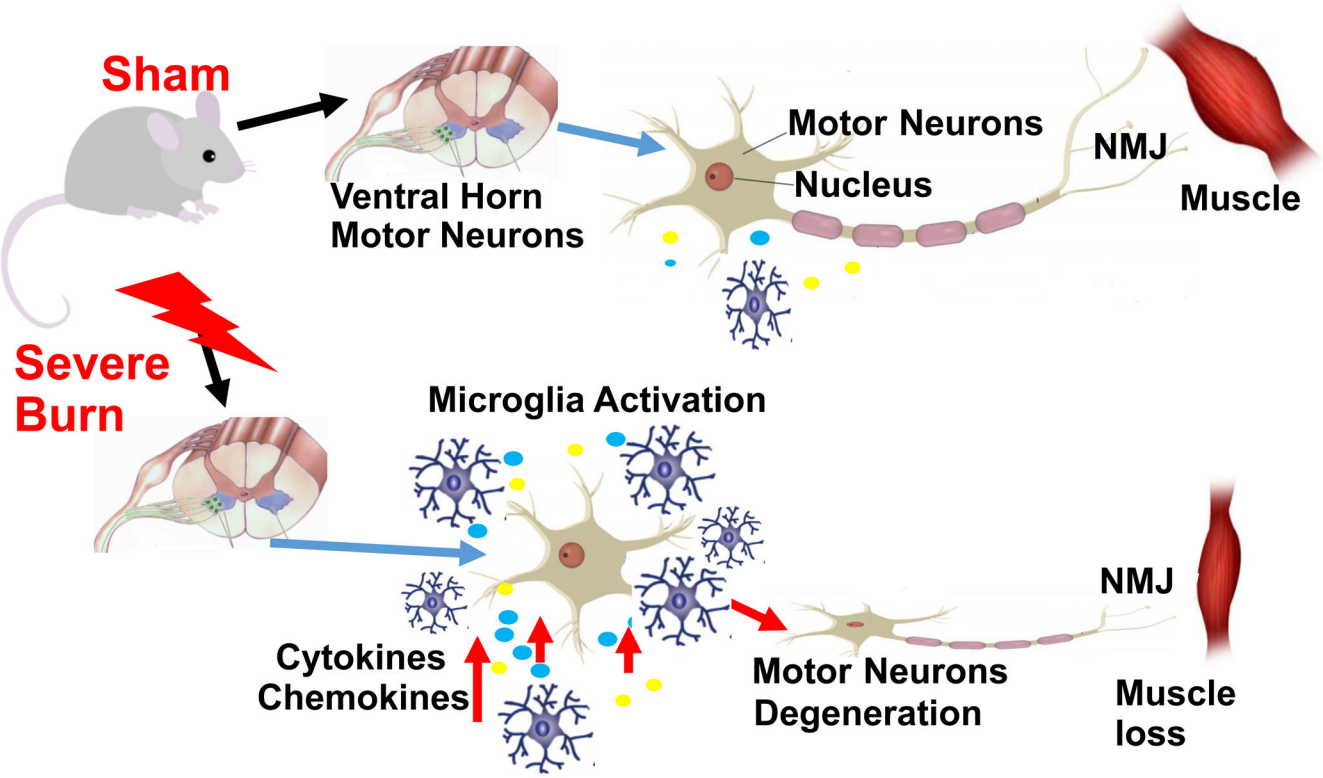

Fig. 6. Schematic diagram of motor neurons and microglia in spinal cord without or with burn injury.

Cartoon of motor neuron unit of SB (normal) (*upper panel*) and BI (*lower panel*) mice. The cartoon demonstrates that in the unburned state that there is minimal microglial activation in the spinal ventral horn and no changes in synapse or muscle mass. Severe BI induces microglia activation in spinal cord ventral horn, evidenced as inflammatory cytokine and chemokine release and is associated with degeneration of motor neurons that correlates to skeletal muscle mass loss.

Table 1.

Primer sequences used for real-time PCR

Target	Primer sequences (5'-3')	Product size (bp)
IL-1β	Forward 5'-GCC CAT CCT CTG TGA CTC AT-3' Reverse 5'- AGG CCA CAG GTA TTT TGT CG-3'	230
IL-6	Forward 5'-AGCCAGAGTCCTTCAGAGA-3' Reverse 5' -TCCTTAGCCACTCCTTCTGT-3'	146
IL-10	Forward 5'-GGT TGC CAA GCC TTA TCG GA-3' Reverse 5'-ACC TGC TCC ACT GCC TTG CT-3'	191
TNF-α	Forward 5' –TGG GAC AGT GAC CTG GAC TGT-3' Reverse 5' - TTC GGA AAG CCC ATT TGA GT-3'	67
CXCL2	Forward 5'-CAG AAGTCA TAG CCA CTCTCAAG-3' Reverse 5'-CTT TCC AGGTCA GTT AGC CTT-3'	119
MCP-1	Forward 5'-GCTCAGCCAGATGCAGTTAA-3' Reverse 5'-TCTTGAGCTTGGTGACAAAAACT-3'	129